Journal of Combinatorial Mathematics
and Combinatorial Computing
www.combinatorialpress.com/jcmcc

Combinatorial Press

Research on Improving the Energy Efficiency of Plasma-Catalyzed Ammonia Synthesis Based on XGBoost and Bayesian Optimization

Jun Du[1], Chunlei Zhang[1], Xin Qiao[1], Lun Li1, Jie Pan[1,] ✉

[1] *School of Physics and Electronics, Shandong Normal University, Jinan, Shandong, 250358, China*

ABSTRACT

Ammonia synthesis is vital for fertilizer production, but the traditional Haber-Bosch process is energy-intensive and environmentally burdensome due to its high-temperature and high-pressure operations. Plasma-catalytic ammonia synthesis offers a sustainable alternative, generating large datasets under various experimental conditions. To optimize energy efficiency, we established a database with 305 data points and 7 experimental parameters, each linked to its corresponding energy efficiency. We employed an Extreme Gradient Boosting (XGBoost) regression tree model, achieving an average R^2 value of 0.9434 for predictions. Bayesian Optimization (BO), using Gaussian Process Regression as a surrogate model, systematically explored the experimental parameter space. It utilized XGBoost predictions to identify parameter combinations that maximized energy efficiency. After 50 iterations, the optimal parameters were identified: 6.4 g catalyst mass, 50 mm grounding electrode length, nickel metal catalyst, Al_2O_3 catalyst support, 5 W power, 160 ml·min^{-1} flow rate, and a 1:2 feed ratio. Under these conditions, the energy efficiency of plasma-catalytic ammonia synthesis improved to 1.49 g·kW·h^{-1}, a 22.1% increase from the highest value of 1.22 g·kW·h^{-1} in the dataset.

Keywords: Plasma Catalysis, Ammonia Synthesis, Dielectric Barrier Discharge, Bayesian Optimization (BO), Gradient boosting regression tree

1. Introduction

Ammonia is one of the most important chemical substances in modern society and is an important raw material for the synthesis of many products [1]. It is widely used in many fields such as petrochemicals, pharmaceuticals, light industry, etc., and its direct downstream products are numerous, such as inorganic nitrogen salts, polyurethane, butyl rubber and its derivatives, etc., of

✉ Corresponding author.
*E-mail address:*xysxzcl@163.com (J. Pan).
Received 03 February 2024; Revised 12 April 2024; Accepted 10 November 2024; Published Online 16 April 2025.
DOI: 10.61091/jcmcc127b-397

which nitrogen fertilizers are one of the most important products [2-4]. In addition, ammonia is a very potential new energy carrier, liquid ammonia has more advantages of high calorific value of combustion, no emission of greenhouse gases and no pollution, which is a green, new type of alternative fuel and will become one of the extremely important sustainable energy sources in the future [5-8]. Nitrogen is a necessary element for the synthesis of ammonia, however, the nitrogen molecule is very stable, resulting in the fact that nitrogen in the air cannot be directly converted and utilized by most living organisms, thus prompting the research and development of artificial nitrogen fixation [9-11].

Ammonia industry is a traditional industry with a hundred-year history, but it is also closely related to new industries such as new coal chemical industry and clean energy [12-13]. As the global energy and environmental conflicts continue to intensify, the ammonia industry is also facing the pressure of reform, and it is an important way to improve the resource utilization rate and enhance energy saving and emission reduction [14-15]. The industrial synthesis of ammonia by the Haber-Bosch method, which requires high temperature and high pressure and is carried out under the action of iron-based catalysts, not only has harsh reaction conditions, but also large-scale production is accompanied by a large amount of energy consumption and greenhouse gas emissions, which has a huge impact on the environment and economic development [16-19]. Therefore, the exploration of new sustainable nitrogen fixation pathways is very necessary.

Due to the harsh reaction conditions of the Haber-Bosch method, which requires high temperatures and pressures, as well as environmental problems, other methods for ammonia synthesis have been developed, mainly including photocatalytic, electrochemical, and plasma methods. Photocatalytic reaction conditions are milder, generally at room temperature and pressure, and the raw materials are mainly from air and water, and energy is provided by a UV-visible light source, which is a green chemical method [20-21]. Zhang, S. et al. presented the research progress and evaluation tools for photocatalytic ammonia synthesis, proposed effective photocatalytic materials as well as reactor design strategies, and also provided practical guidelines for performance evaluation of catalysts and ammonia detection methods [22]. Ithisuphalap, K. et al. showed that photochemical synthesis of nitrogen reduction is a sustainable method for ammonia production and addressing the material, structural and morphological defects faced by the photocatalysts in this reaction is the main challenge to improve the photoreduction performance of nitrogen [23]. Shi, Y. et al. explored the design and preparation paradigm of catalysts in photocatalytic ammonia synthesis in terms of materials, structures, and reaction engineering with the aim of improving the reaction efficiency of photocatalytic ammonia synthesis [24]. Zhao, Z. et al. established a bimetallic organic framework to realize the decoupling of electron accepting and giving processes in photocatalytic ammonia synthesis, which is conducive to the activation of nitrogen chemical bonding activation energy, as well as the enhancement of photocatalytic activity [25]. However, due to the limitation of low nitrogen activity, the target product yield of photocatalytic ammonia synthesis is still far below the requirement in practical applications.

Electrochemical synthesis of ammonia via nitrogen reduction reaction (NRR) driven by renewable energy sources under mild conditions is an attractive approach that has received a lot of attention in the last few years [26-27]. Yao, Y. et al. revealed that electrochemical synthesis of ammonia under mild conditions is based on the principle of converting renewable electrical energy into chemical energy in the form of ammonia, and that the synthesis efficiency of this process is affected by a number of factors such as catalytic material and reaction process [28]. Wu, T. et al. pointed out that electrochemical synthesis of ammonia not only has great economic and environmental benefits, but also has outstanding advantages in industrial production by reducing nitrogen-containing pollutants to produce ammonia [29]. Yang, J. et al. examined the electrochemical synthesis of ammonia gas in molten

salts to optimize the composition of ammonia and molten salts and to add suitable electrocatalysts to achieve an increase in the efficiency of ammonia synthesis from molten salts under scale-up conditions [30]. Kyriakou, V. et al. analyzed the application of electrochemical methods for ammonia synthesis in solid and liquid electrolyte cells and compared the techno-economic advantages and limitations of electrochemical methods compared to other methods, aiming to maximize the requirements for ammonia synthesis in industrial production [31]. Despite the progress made in the field of electrochemical ammonia synthesis in the above studies, finding more suitable catalysts or improving the activity, selectivity, and stability of the existing catalysts are the main challenges to be faced.

Plasma synthesis of ammonia is considered to be a promising alternative to thermocatalytic ammonia synthesis because of the advantages of ultra-fast reaction time, mild reaction conditions, controllable reaction, and better integration with other technologies [32-33]. Zhu, X. et al. investigated the effect of different catalysts on the post-reaction ammonia yield and energy efficiency in a dielectric-blocked discharge plasma reactor, and found that the structure of the catalytic and has a strong connection with the reaction performance of the plasma ammonia synthesis system [34]. Hosseini, H. focused on the advantages of non-thermal medium blocked discharge plasma in ammonia synthesis systems, which has a higher potential for application due to higher generation efficiency and energy efficiency compared to normal plasma ammonia synthesis systems, as well as facilitating the control of by-products [35]. Kim, H. H. et al. examined the ammonia synthesis reaction over a ruthenium catalyst by atmospheric pressure low-temperature plasma, and the efficiency of ammonia synthesis could be effectively improved by varying the gas ratio of the N2-H2 mixture as well as the temperature at which the reaction took place [36]. Sun, J. et al. illustrated the kinetic mechanism of nanosecond pulsed discharge plasma in an ammonia synthesis system, which improves the kinetic ammonia generation efficiency of the system by increasing the coupling of the catalyst and the plasma, as well as providing new insights into the roles of the excited state and the plasma-enhanced surface chemistry [37]. Rouwenhorst, K. H. et al. explored the green ammonia synthesis method under plasma-driven conditions, investigated the ammonia synthesis mechanism under different plasma and presence or absence of catalyst conditions, respectively, and analyzed its limitations to provide a reference for the complexity of the ionophore-catalyzed ammonia synthesis reaction [38]. Non-thermal plasma technology offers a promising pathway for ammonia synthesis, where plasma combined with catalysts can substantially increase the rate of ammonia synthesis as well as the energy yield. Therefore, optimization of the energy efficiency of plasma-catalyzed ammonia synthesis will play a very important role in guiding industrial ammonia production.

In this paper, an optimization method combining BO and XGBoost models is proposed to determine the experimental parameter combination that maximizes the energy efficiency of plasma catalyzed ammonia synthesis in a limited experimental parameter space. A dataset of seven widely studied experimental parameters and their corresponding energy efficiency was constructed based on the literature screened from 2021 to 2024. The XGBoost model was trained using this data set to predict the energy efficiency of plasma catalyzed ammonia synthesis and then used to construct the BO objective function. By selecting the optimal proxy model and conducting 50 iterative searches, BO finally identifies the experimental parameter combination that achieves the highest energy efficiency and verifies it with the dynamic model. Finally, the trained XGBoost model is used to explore the relationship between experimental parameters and energy efficiency to further verify the BO results.

2. Method

Figure 1 is the flow chart of optimization of experimental parameters of plasma catalyzed ammonia synthesis combined with BO and XGBoost models. The method framework in this paper mainly

includes three steps: data processing, XGBoost model construction and BO iteration. First, the experimental data are collected and pre-processed to train the XGBoost model to predict the relationship between experimental parameters and energy efficiency. Secondly, BO iteration is used to optimize the energy efficiency based on the trained model. After the number of iterations is reached, the maximum energy efficiency and the corresponding experimental parameter combination are output.

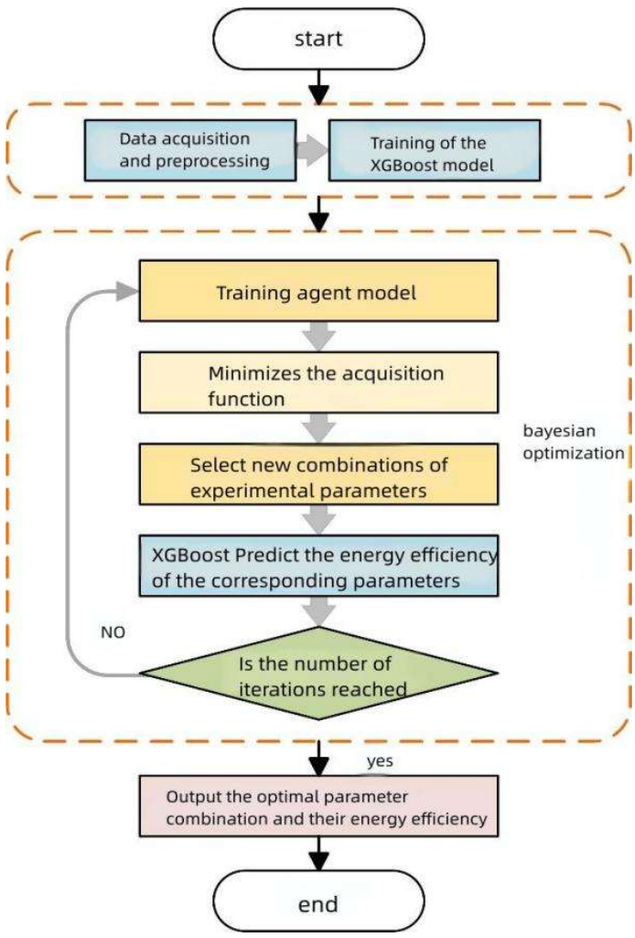

Fig. 1. Optimization Process for Experimental Parameters in Plasma Catalysis of Ammonia Synthesis Combining Bayesian Optimization and XGBoost Model

2.1. Dataset construction

This paper focuses on experimental studies using DBD reactors under normal temperature and pressure conditions, selects relevant literature from 2021 to 2024, and manually collects 7 widely studied experimental parameters and their corresponding energy efficiency data. In the end, a dataset of 305 data points and 8 parameters was built.

2.1.1. Plasma-catalyzed synthetic ammonia reaction system. The database constructed in this paper is based on selected core literature on plasma catalyzed ammonia synthesis from 2021 to 2024. The experimental studies in these literatures all adopted DBD reactors under normal temperature and pressure conditions, and the reaction systems have a high degree of similarity, which ensures the unity and comparability of data sources. Figure 2 shows a schematic diagram of the reaction system. Plasma catalytic ammonia synthesis experiments were carried out in a DBD reactor, which was sealed by two

polytetrafluoroethylene (PTFE) seals. The high voltage electrode is a stainless steel rod connected to the AC pulse power supply, and the ground electrode is a fixed length copper network outside the reactor. The voltage probe is used to monitor the relevant voltage, and the signal is recorded by the oscilloscope. When plasma catalyzed ammonia synthesis is carried out, the discharge area is filled with catalyst or pure carrier. High purity nitrogen (99.999%) and hydrogen (99.999%) were pre-mixed at the corresponding flow rate and introduced into the DBD reactor at atmospheric pressure for PCAS. Fourier transform infrared spectrometer was used to detect the composition and proportion of the gas products. Before the product gas entered the gas chamber of the spectrometer, the flow rate of the product at the outlet of the reactor was measured by a flowmeter.

In this paper, the DBD reactor limited to normal temperature and pressure is selected for the following reasons. Firstly, the DBD reactor can produce non-equilibrium plasma efficiently, and the non-equilibrium interaction between its high-energy electrons and low-temperature ground state molecules helps to significantly reduce the activation energy of ammonia synthesis reaction. Secondly, compared with the traditional high-temperature and high-pressure reaction conditions, the DBD reactor is operated at normal temperature and pressure, which has low energy consumption, high safety, and easier to regulate and reproduce the experimental conditions. The most important is that the DBD reactor has strong adaptability and can flexibly combine different catalysts and parameters, which provides an ideal platform for studying the mechanism of the synergistic interaction between plasma and catalyst.

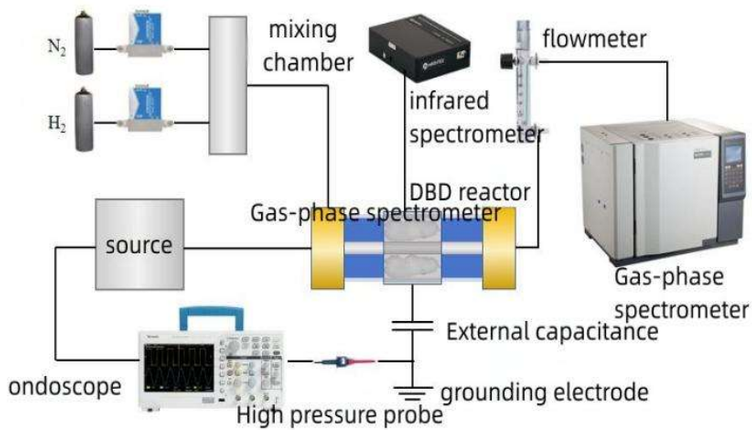

Fig. 2. Schematic Diagram of the Plasma-Catalyzed Ammonia Synthesis System

2.1.2. Selection and acquisition of feature parameters. In the plasma catalyzed ammonia synthesis reaction system, many parameters affect the reaction process and system performance. In order to scientifically and reasonably select the parameters that can fully characterize the characteristics of the system, it is necessary to evaluate and analyze with the help of some key quantitative indicators. Power, specific energy input and energy efficiency can reflect the energy input, distribution and transformation of the system, and provide a basis for the selection of characteristic parameters. Power is the key factor affecting energy input and reaction efficiency. The calculation formula is:

$$P_d\,[W] = f \cdot C_{ext} \cdot A \tag{1}$$

The f represents the pulse frequency of the power supply, the C_{ext} is the capacitance of the external capacitor, and the A is the pulse period of the Lisa as a graphical area.

The specific energy input represents the energy received by the reactant per unit volume, which describes the distribution of the input energy in the reactant and affects the energy state of the

reactant molecule. Different specific energy input will make the reactant molecule in different excited states, which plays an important role in the start and continuation of the reaction. The calculation formula is:

$$SEI\left[\mathrm{kJ/L}\right]=\frac{60\cdot P_d}{Q} \tag{2}$$

Q(mL/min) represents the total flow rate of the premixed gas.

Energy efficiency is the ratio of the mass (g) of ammonia produced by the synthesis of ammonia to the electricity consumed (kWh). A higher energy efficiency means that more ammonia products can be obtained for the same energy input. The calculation formula is:

$$E_{\mathrm{NH_3}}\left[\mathrm{g/kWh}\right]=\frac{60\cdot 17\cdot Q\cdot C}{24\cdot 1000000\cdot P_d} \tag{3}$$

Where the coefficient "17" indicates the molar mass of the ammonia, and "1,000,000" is the unit conversion coefficient. C (ppm) represents the ammonia concentration of the product gas.

Based on the operable variables of the reaction system and the above formulas of power, specific energy input and energy efficiency, some parameters for characterizing the system characteristics, including catalyst mass, grounding electrode length, power, gas flow rate and feed ratio, are preliminarily determined. Considering that all the catalyst types used in the selected experimental devices are all metal-loaded catalysts, this paper innovatively uses active metal and catalyst carrier to identify the catalyst. Active metal is the key site of catalytic reaction, and its type and nature determine the activity and selectivity of the reaction, by affecting the dispersion and stability of active metal. The collected parameters and values are summarized in Table 1, including 7 experimental parameters and their corresponding energy efficiencies, and all the data were collected through the "Pick Data Points" tool of Origin software.

2.1.3. Feature encoding and data preprocessing. In order to ensure that the model can accurately identify and effectively use non-numerical parameters, the active metal and catalyst carrier should be encoded. For active metals, atomic numbers are encoded and considered as categorical variables. The atomic number of the active metal can directly reflect its specific position in the periodic table and its basic properties. Through this encoding method, the category information of active metals is retained. For catalyst carriers, this label coding method is used to convert the discrete catalyst carriers into a numerical format. The label coding maps the category of the catalyst carriers into a unique integer value, and each carrier category is assigned a unique integer value. For experiments without catalyst carriers, their corresponding category values were uniformly labeled as 0 to ensure data integrity and consistency. After encoding processing, each data point in the database is transformed into a vector containing experimental parameters and energy efficiency, where the experimental parameters include the numerical results of the discrete parameters and other numerical parameters.

After encoding of non-numerical parameters, the whole dataset was standardized to eliminate dimensional differences between different parameters and lay a consistent data foundation for subsequent model training and optimization algorithm application. In this paper, the Z-score standardization method, which subthe mean value from each parameter value and divides by the standard deviation, transforms the data into a distribution with mean of 0 and standard deviation of 1, the formula is as follows:

$$z=\frac{x-\mu}{\sigma} \tag{4}$$

Table 1. The collected parameters and their values

argument	value
metal	Nickel, iron, ruthenium, copper, cobalt
Catalyst support	Al2O3、BaTiO3、γ-Al2O3、Si-MCM-41、SiO2、AC、ZSM-5、α-Al2O3
Catalyst mass /g	0.18~12
Grounding electrode length /mm	8~50
Power /W	5~67
Gas flow rate /ml·min-1	20~160
Nitrogen and hydrogen feeding ratio	1:5、1:3、1:2、1:1、2:1、3:1、5:1
Energy efficiency/g·kW·h^{-1}	0.05~1.22

z is the normalized values, x is the original parameter values, μ is the mean value of this parameter, σ is the standard deviation of this parameter.

Through the correlation analysis, we plot the experimental parameter correlation heat maps in Figure 3 to show the relationship between these parameters. Most of the correlation coefficients in the thermal maps are low, which proves that the present dataset covers a broad and diverse information sources that contribute to the comprehensive understanding and characterization of the processes of ammonia synthesis catalyzed by plasma. The low correlation coefficient indicates a relative independence between the selected parameters, meaning that each parameter may capture the unique aspects affecting the ammonia synthesis process in plasma catalysis. This independence avoids the problem of multicollinearity, namely that multiple input variables are highly correlated, which may lead to instability and interpretation difficulties during model training. From Figure 3, we can see that the correlation between most parameters have weak or no significant correlation. The correlation between the metal species and the catalyst carrier is only 0.19, indicating that these two factors have little influence on each other. Similarly, the correlation of energy efficiency and other parameters is equally insignificant, which further confirms the importance of each parameter to the predicted target and its unique contribution.

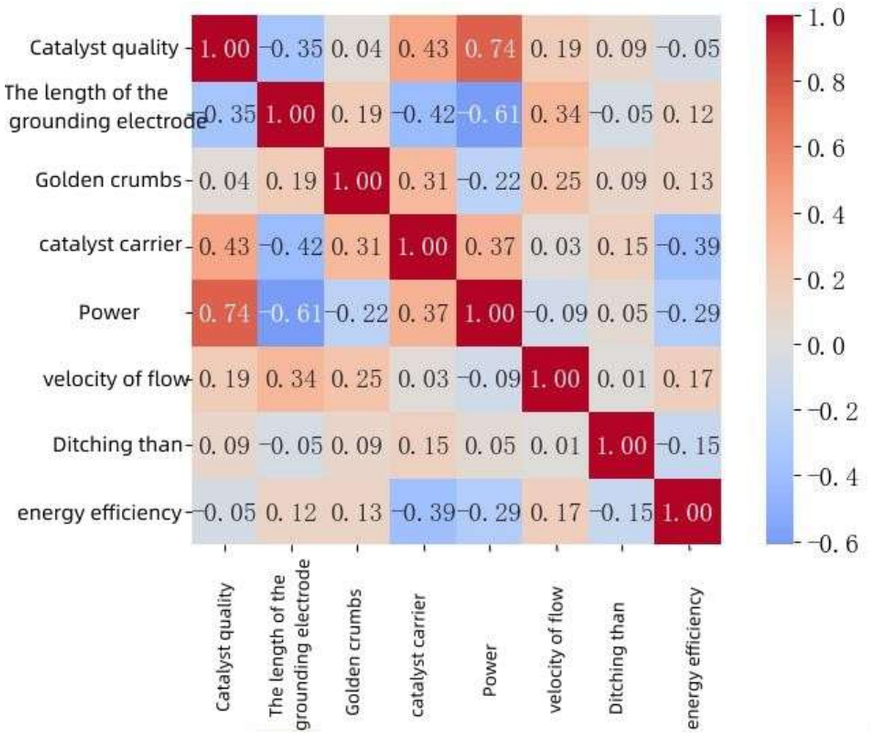

Fig. 3. Correlation heatmap of experimental parameters

2.2. XGBoost Regression model construction and training

Before optimizing the experimental parameters of the catalyzed ammonia synthesis of plasma, it is necessary to train a model that accurately predicts the energy efficiency instead of traditional software simulation or practical experiments to construct the objective function of BO and achieve efficient evaluation of candidate parameter combinations during the BO process.

XGBoost is an advanced ensemble learning algorithm to builds efficient prediction model by integrating multiple weak learners. The algorithm adopts a step-wise fitting method to improve the model prediction accuracy by correcting the prediction error left by the previous weak learner. XGBoost Not only consider the traditional loss function and model complexity when constructing the objective function, but also introduces regularization terms to effectively prevent overfitting, thus enhancing the computational performance and prediction accuracy of the model. XGBoost Good at dealing with non-linear problems, with its strong generalization ability, excellent performance in various classification and regression tasks, so it has been widely used.

The constructed dataset is given as follows $D=\{(x_i,e_i)\}(i=1,2,\ldots,n)$, x_i and e_i are the experimental parameters and the energy efficiency, respectively. Suppose that training a model with k trees. Forecast results (e_i) as follows:

$$\hat{e}_i=\sum_{k=1}^{K}f_k(x_i),\quad f_k\in \mathrm{F} \tag{5}$$

The objective function expression to be optimized is as follows:

$$Obj=\sum_{i=1}^{n}L(e_i,\hat{e}_i)+\Omega \tag{6}$$

$\sum_{i=1}^{n}L(e_i,\hat{e}_i)$ is the training loss function, Ω represents the complexity of the model.

After completing the construction of the XGBoost model, BO is further used to optimize the hyperparameters of the model to improve the overall performance of the model. The hyperparameters that need to be optimized are shown in Table 2. The data set was divided into the training set and the test set in a ratio of 8:2. In the model training stage, 50% off cross-validation is used to make full use of the data and reduce the evaluation bias due to the randomness of data division. That is, the database is divided into five non-overlapping subsets, and the model is trained with four subsets in turn, with a remaining subset as the validation set. This process is repeated five times. The determination coefficient (R-Square, R2) is used as the evaluation index, and the expression is:

$$R^2 = 1 - \frac{\sum_{i=1}^{n}(\hat{e}_i - e_i)}{\sum_{i=1}^{n}(e_i - \overline{e})} \tag{7}$$

Where $e_1, e_2, \ldots, e_n$ is the true value, $\hat{e}_1, \hat{e}_2, \ldots, \hat{e}_i$ is the predicted value, $\overline{e}$ is the average of these true values, n Represents the sample size of the training or test phase. Model performance is optimized by minimizing the error between the predicted and actual values to improve the accuracy of prediction energy efficiency. To ensure that the model can adequately learn the data features and effectively avoid overfitting, 100 iterations were set.

Table 2. Description of hyperparameters

hyperparameter	span	Initial value
n_estimators	[10, 200]	100
learning_rate	[0.01, 0.3]	0.1
max_depth	[1, 10]	5
min_child_weight	[1, 10]	5
subsample	[0.5, 1]	0.5
colsample_bytree	[0.5, 1]	0.5

2.3. The Bayesian optimization algorithm

Recently, as a data-driven method, BO has been widely used as an efficient parameter search method to search for parameter that satisfy specific properties. BO usually involves two main steps: the learning stage and the optimization stage. In the learning phase, BO updates the agent model with each iteration, gradually approaches the “best guess” of the relationship between the objective function and the design parameters, and quantifies the uncertainty of this guess. In the optimization phase, an acquisition function is selected to guide the optimization process, and the next point to be evaluated (i. e., the combination of experimental parameters) is determined by maximizing the acquisition function value. The goal of choosing this is to balance exploration and development, usually using the desired improvement (EI, expected improvement) as the acquisition function.

The specific process of BO exploring the ammonia parameter space is as follows: first, some experimental parameters are randomly selected and the initial energy efficiency is obtained through the XGBoost regression model; then the BO framework trains the agent model from the existing data set and recommends the next set of parameters to be evaluated through the acquisition function; then the recommended parameter combination is input into the XGBoost model to obtain the predicted energy efficiency, and it is added to the data set and used to update the agent model. The process is repeated until a preset number of iterations is reached.

An important innovation of this paper lies in the application of BO to the optimization of

experimental parameters of plasma catalytic ammonia synthesis, especially considering the special case that metal, catalyst carrier and feed ratio are categorical variables. In the past, in the field of parameter optimization, most algorithms usually focus on the treatment of continuous variables, but there are some limitations in the optimization of categorical variables. The BO algorithm used in this paper shows a unique advantage of effectively dealing with the classification variables of metal, catalyst carrier and feed ratio. In addition, three commonly used proxy models are compared, including random search, random forest regression, and Gaussian process regression. In this paper, we will compare the energy efficiency maximum achieved by the three proxy models with the same number of iterations, and choose the best proxy model to drive the process of BO optimizing the experimental parameters of ammonia synthesis by plasma catalysis. In this paper, the code runs in the Python 3.8.0 environment, and the XGBoost model is implemented with the xgboost 1.15.0 library, and the scikit-optimize library is used to carry out BO related work.

3. Results and Discussion

3.1. XGBoost Model training results

3.1.1. Comparison and selection of the regression models. In this paper, four regression models, XGBoost, KNR, SVM and ANN, were tested to determine the best prediction model. As shown in Figure 4, the four models show different performance in terms of energy efficiency prediction. Although the predicted value of KNR model coincides with the actual value curve to a certain extent, there is significant deviation at multiple sample points, and the prediction error is relatively obvious, and the error of some sample points even exceeds 0.25. Similarly to the SVM model, where the number of sample points is 10 to 20 and 40 to 50, the prediction error is particularly prominent, and it is difficult to accurately track the change trend of the actual value. The fluctuation characteristics of the predicted value of ANN model are quite different from those of the actual value curve, and the actual value cannot be effectively fitted in multiple sample points, resulting in the lack of stability of the prediction error and the difficulty to provide reliable energy efficiency prediction results. In contrast, the XGBoost models perform very well. The predicted value almost completely coincide with the actual value curve. In the whole sample interval, the deviation between the predicted value and the actual value is very small, the prediction error is always maintained at a low level, and the error of most sample points is controlled within 0.05. It is thus determined that the XGBoost model is the best model for predicting energy efficiency.

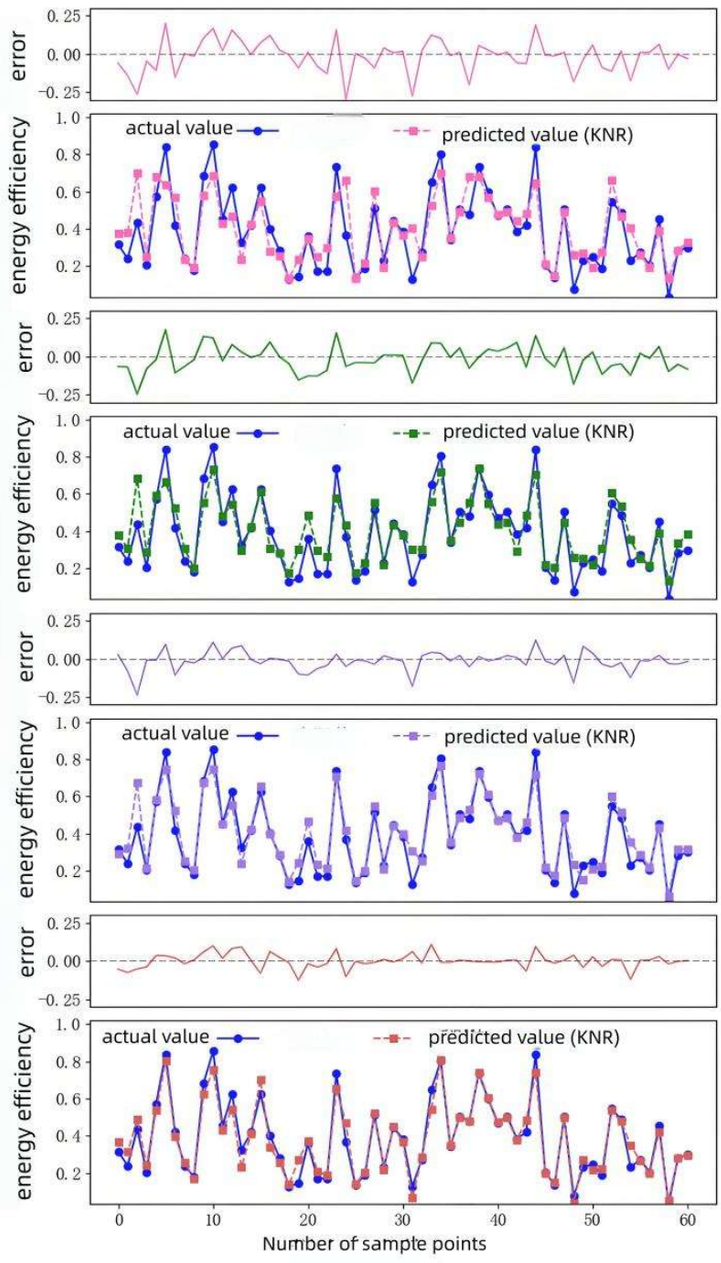

Fig. 4. Performance Evaluation of Energy Efficiency Prediction Models Based on XGBoost, KNR, SVM, and ANN

3.1.2. XGBoost Hyperparameter optimization of the model. To further improve the accuracy of the XGBoost model in the energy efficiency prediction, the hyperparameters of the model were optimized using BO, and the results are shown in Table 3. The number of trees was determined as 117, and this parameter had important effects on the complexity and predictive power of the model. The learning rate is set to 0.2304 to balance the learning speed and model stability; the maximum depth of the tree is set to 3 to prevent overfitting to enhance the generalization ability of the model; the minimum node weight is set to 1 to control the minimum sample weight of each leaf node to further suppress overfitting; the sample sampling ratio is 0.7911 to indicate the sample proportion used to train the model in each iteration; the feature sampling ratio is 0.6, which specifies the feature proportion randomly sampled for each tree.

Following the hyperparameter optimization, the prediction performance of the XGBoost model is next evaluated. Figure 5 shows the comparison of the predicted value of the energy efficiency of ammonia synthesis in the XGBoost model before and after hyperparameter optimization. The abscissa represents the true value of the energy efficiency of plasma-catalyzed ammonia synthesis, the ordinate indicates the corresponding predicted value, and the dashed line indicates the ideal predicted line, representing the trend when the predicted value is completely consistent with the true value. The circles represent the optimized data points, and the triangles represent the data points before the optimization. It can be seen that the circular points are relatively concentrated around the ideal prediction line, and the R^2 value reaches 0.9434, which indicates that the XGBoost model has extreme prediction accuracy after hyperparameter optimization

Big ascension. The application of XGBoost model in the risk assessment of highway tunnel instability and showed that the model achieved an overall accuracy rate of 93.75% in the risk assessment, which was consistent with the high R^2 value of the paper, further confirming the stability and reliability of XGBoost in handling complex problems.

Table 3. Hyperparameter Optimization Results

hyperparameter	meaning	short-cut process
n_estimators	The number of trees	117
learning_rate	Learning rate	0.2304
max_depth	The maximum depth of the tree	3
min_child_weight	Minimum child node weight	1
subsample	Sample proportion	0.7911
colsample_bytree	Feature sampling ratio	0.6

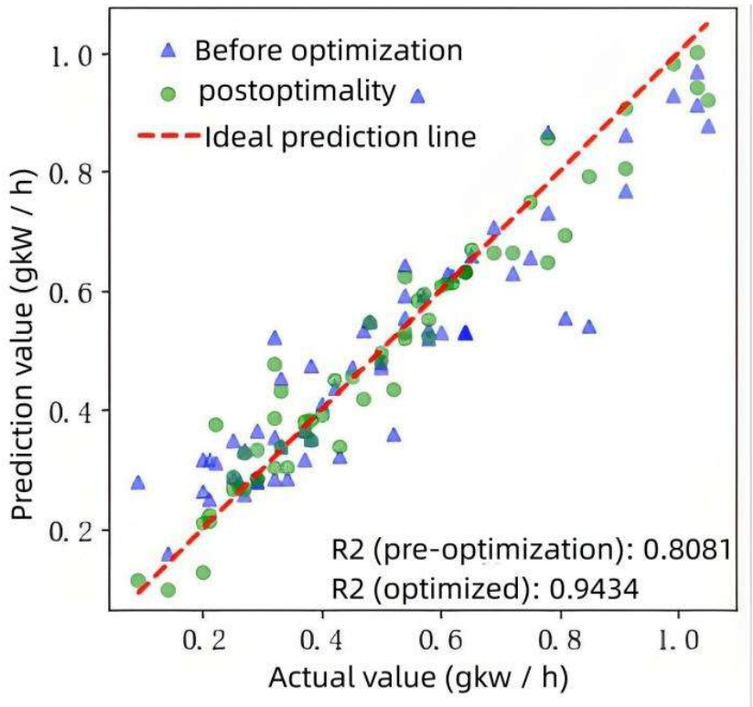

Fig. 5. Comparison Chart of XGBoost Models Before and After Hyperparameter Optimization

3.2. Analysis of the results of the Bayesian optimization

3.2.1. Comparison of the agent models. This subsection compares the effects of the three agent models in the optimization process. Figure 6 is a comparison diagram of the BO search process of the three agent models. The horizontal axis represents the number of searches, and the vertical axis is the historical maximum energy efficiency achieved by the current number of searches. Gaussian process regression is the best performance, thanks to its strong modeling ability and accurate expression of uncertainty. Through the mean function and the covariance function, the Gaussian process regression can dynamically fit the objective function, and effectively balance the exploration and development. As can be seen in the figure, after about 20 searches, the Gaussian process regression quickly approaches the optimal value, and then the change range is very small, showing the optimization ability of rapid convergence and stability. This paper further verified that the Gaussian process has become a widely used proxy model in BO because of its recursive modelling properties, showing better optimization effects.

In contrast, random forest is better in some rounds, but the overall process is slow. Random forest is essentially an integrated model of multiple decision trees, with strong local optimization ability, but the global search efficiency is not optimal. Moreover, it fails to provide continuous prediction with uncertainty measures as in Gaussian process regression, limiting its optimized performance in the high-dimensional parameter space. The optimization efficiency of random search is the lowest, because it adopts the pure random search method, does not use the existing sample information to guide the search direction, and only relies on random sampling, resulting in very low search efficiency. Moreover, due to the lack of modeling ability of the objective function, the stochastic search completely depends on the random collision optimal region during optimization, and the convergence curve is slow and unstable.

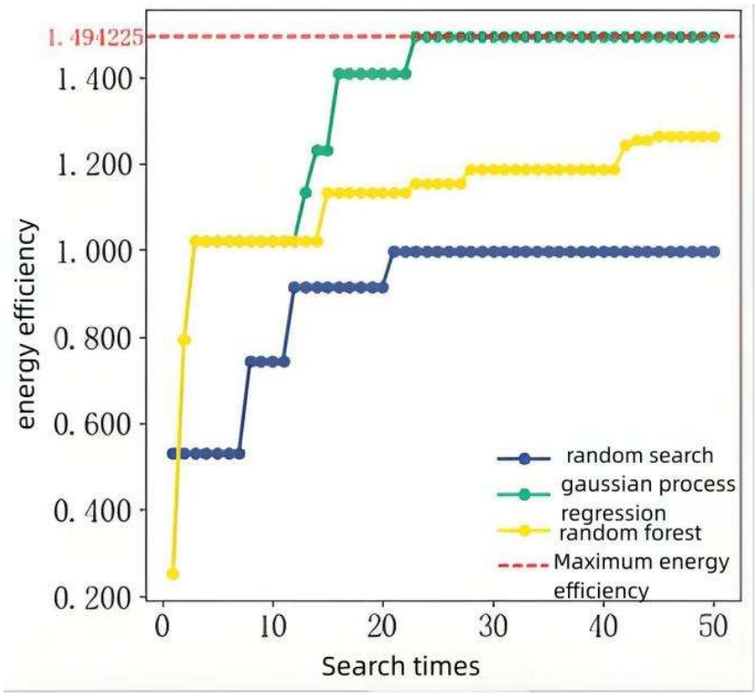

Fig. 6. Comparison of BO search processes using three different surrogate models

3.2.2. Search results for 50 iterations of Bayesian optimization. Gaussian process regression was chosen as the proxy model according to the results in Section 2.2.1. Figure 7 shows the parameter combination obtained with 50 iterations. Each curve represents a different combination of experimental parameters used for one optimization iteration, and the color depth of the curve corresponds to the change of the objective function value, i. e., the energy efficiency. BO gradually converges with an increasing number of iterations, indicating that BO is able to rapidly approximate the optimal solution with a finite number of experimental iterations. In the early stage of optimization, BO mainly focuses on exploring the unknown potential optimization areas, while in the later stage, the parameters are adjusted more carefully, so as to achieve the accurate approximation of the optimal solution.

Based on the results of BO iterative search, the best experimental parameters for ammonia synthesis are: the catalyst mass is 6.4 g, the length of grounding electrode is 50 mm, the nickel is selected as the metal catalyst, Al_2O_3 is used as the catalyst carrier, the power is 5 W, the gas flow rate is 160 ml·min^{-1}, and the feed ratio of nitrogen and hydrogen is set at 1:2. Under this condition, the energy efficiency reached 1.49 g·kW·h^{-1}, which shows a significant improvement of about 22.1% compared with the highest energy efficiency of 1.22 g·kW·h^{-1} recorded in the dataset.

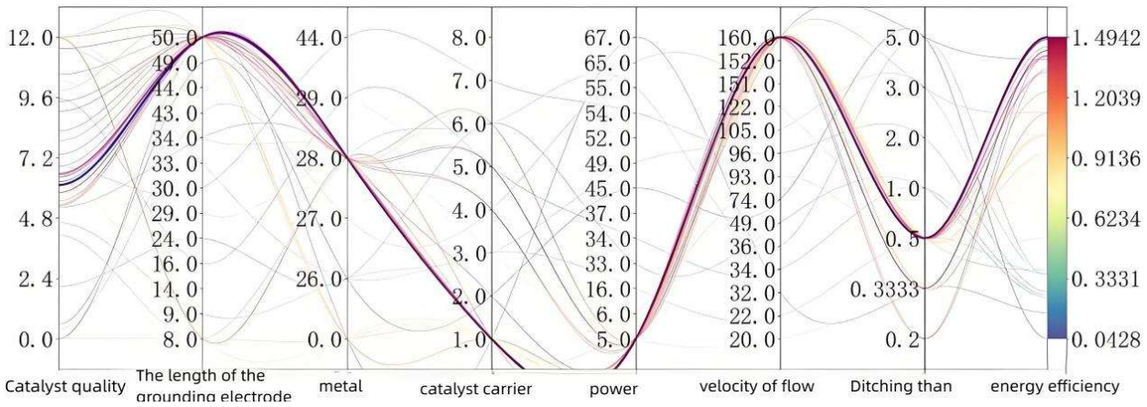

Fig. 7. The parameter combinations obtained by BO search with 50 iterations and the corresponding changes in energy efficiency

3.3. Results for the validation of the optimal parameter combination

The resulting optimal combination of experimental parameters is embedded in the gas phase-surface coupling dynamics model based on ZDPlaskin solver. By updating the surface reaction equation and the corresponding rate coefficient of the nickel-based catalyst, the parameters such as gas flow rate and nitrogen-hydrogen ratio were adjusted to the optimal parameter combination value obtained by BO, and the power was set at 5W, 15W, 25W and 35W respectively. Under this condition, the ammonia concentration of plasma-catalyzed ammonia synthesis is obtained by simulation, and the energy efficiency under the corresponding conditions is obtained by calculating formula (3). At the same time, the above adjusted parameters are input into the XGBoost model for operation to obtain the predicted energy efficiency.

The results are shown in Figure 8, although the predicted and simulated energy efficiency differ in specific values, but the overall trend is the same. It is evident from the figure that, as the power gradually increases from 5W to 35W. The predicted energy efficiency decreased from 1.49 g·kW·h^{-1} to 1.19 g·kW·h^{-1}, and the simulated energy efficiency decreased from 1.38 g·kW·h^{-1} to 1.08 g·kW·h^{-1}.Both showed a trend of decreasing with increasing power. This suggests that the predictions and simulations are consistent in the trend of the response to power changes.

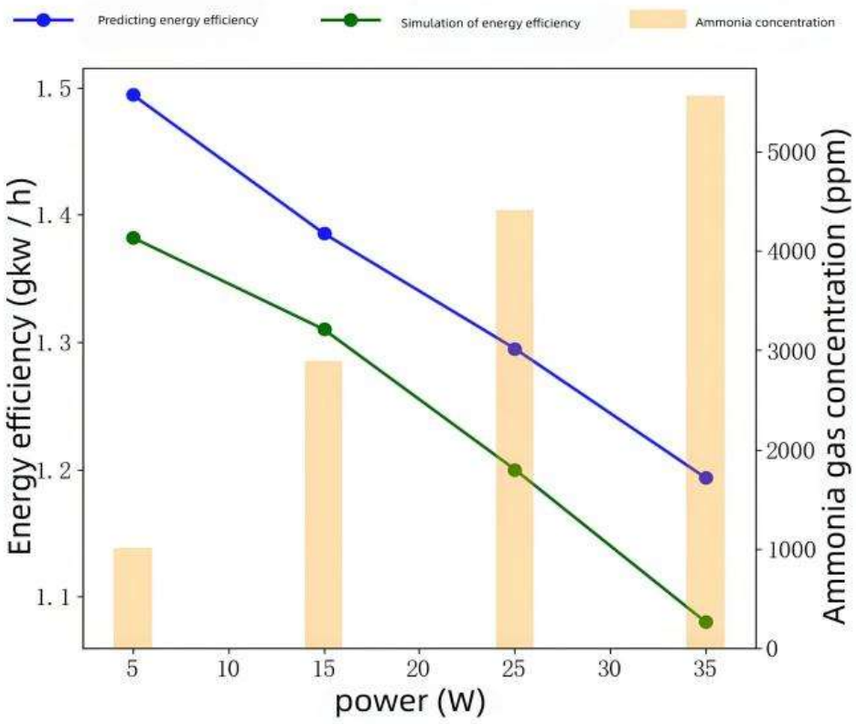

Fig. 8. Comparison of Predicted and Simulated Energy Efficiencies and Ammonia Concentrations in Plasma-Catalyzed Ammonia Synthesis under Different Powers three different surrogate models

By calculating formula (3), the maximum energy efficiency of the numerical simulation result is 1.382 g·kW·h^{-1},, which is somewhat different from the predicted 1.49 g·kW·h^{-1}, but within a reasonable range. This is mainly derived from the diverse complexity of the data sources. On the one hand, the collected data comes from different experimental devices, and there are many detailed differences in the structure, material, internal structure and other aspects. The length, diameter and roughness of the gas transmission pipeline of different devices may affect the uniformity and stability of the gas flow rate, and then affect the reaction process. On the other hand, the numerical simulation itself is an approximation of the response to reality. Although the model tries to consider various factors, it is inevitable that some small factors that work in the complex realistic environment will be ignored in the actual verification process. For example, trace impurities in the actual reaction system may not be fully considered in numerical simulations because they are difficult to quantify accurately, but they may have some influence on the energy efficiency in the actual reaction. Combining these factors, the error between the simulated and predicted values is within a reasonable range, further proving the effectiveness of the optimization scheme.

3.4. Analysis of the effect of the experimental parameters on the energy efficiency

In this section, the trained XGBoost model is used to explore the relationship between the experimental parameters and the energy efficiency to further validate the BO results. Figure 9 shows the results of the SHAP value analysis of the XGBoost model. Positive SHAP value indicates a positive effect on energy efficiency, the higher the value, the higher the effect of improvement, and negative SHAP value means that the parameter has a negative effect on energy efficiency. From the SHAP value in Figure 9, each parameter is ranked from high to low by metal, power, catalyst quality, catalyst support, flow rate, length of grounding electrode, and feed ratio.

Figure 10 shows the trend of SHAP values for the influence of each experimental parameter on energy efficiency. It can be found that with the increase of catalyst quality, the energy efficiency increases and then decreases. When the catalyst quality is low, the increase quality will improve the energy efficiency by providing more active sites, while when the quality is too high, the agglomeration and system physical properties change hinder mass transfer, thus reduces the energy efficiency; as the grounding electrode length increases, the energy efficiency decreases first and then increases. In the range of 10-30mm, the energy efficiency is significantly reduced, because the short electrode concentrates the electric field, but the reactant contact opportunity is insufficient. When the electrode becomes longer, the electric field distribution in the reaction area is more uniform, the reaction surface area increases, more reactants participate in the reaction, and the energy utilization rate can be improved. This paper found a U-shaped curve of NH_3 concentration and energy efficiency when the electrode length was increased, which is consistent with the trend presented in some related research.

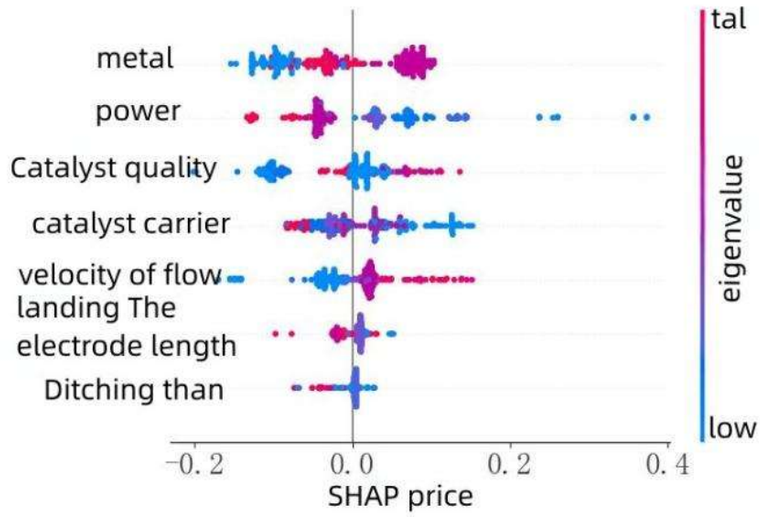

Fig. 9. Analysis Results of SHAP Values for XGBoost Model

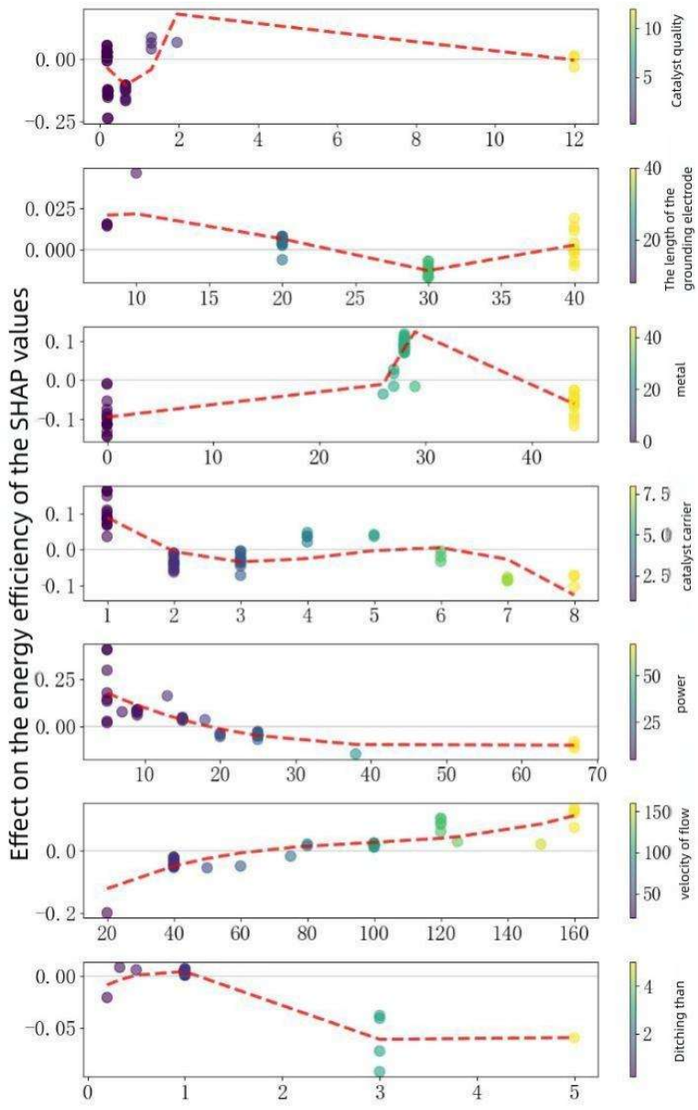

Fig. 10. Analysis of the Effects of Various Factors on Energy Efficiency Based on SHAP Values

Metals achieve higher energy efficiency at the atomic number of 28, or nickel. Nickel has obvious advantage as active metal. Nickel electron configuration is conducive to electron exchange and adsorption with the reactants, and the complex reaction performance is better than iron, cobalt, copper and ruthenium. Moreover, nickel has good dispersion and high thermal stability, which can effectively prevent sintering and inactivation. Al_2O_3 coded as 1 is more efficient when loaded as a catalyst, because it is due to its good mechanical properties, stress resistance, complete structure and large specific surface area, which is conducive to the dispersion of active metals and increases the contact between the reactants and the active site. The energy efficiency gradually decreases as the input power increases. This is because excessive ionization triggers side reactions and reduces the efficiency of ammonia generation. Moreover, the trend shown in this paper found that the increased proportion of electron energy waste at high power leads to a decrease in energy utilization.

As the gas flow rate gradually increases, the energy efficiency increases. With the increase of flow rate, the gas molecules pass through the plasma region per unit time, which makes the effective collision possibility of N and H reaction species increases, which improves the synthesis performance

of NH_3. The present found that a higher flow rate can improve the reaction efficiency in the methane dry reforming reaction, namely, accelerating the speed of the reactant through the reaction zone helps to reduce the side reaction. When the feeding ratio is 1, the energy efficiency reaches a greater value. When N2 and H2 are fed at 1:1, the collision frequency and effective collision probability between them reach the optimal state, which can be efficiently converted into ammonia gas.

4. Conclusion

Here, we present a method for optimizing the experimental parameters of the plasmonic catalytic synthesis of ammonia by combining BO to the XGBoost model. Energy efficiency was predicted using XGBoost regression models by constructing a database of 305 experimental data points. Based on this, BO was applied to systematically search for experimental parameters and finally determine the best combination of experimental parameters. The main conclusions are summarized as follows:

1) In predicting the energy efficiency of plasma catalytic ammonia synthesis, XGBoost has excellent performance with R^2 of 0.9434, which is higher than the KNR, SVM and ANN models under the same test conditions. This indicates that XGBoost can more effectively capture inter-variable relationships with higher prediction reliability and accuracy.

2) According to the systematic search of the parameter space, BO identified the best parameters: the weight of the catalyst was 6.4g, the length of the electrode was 50mm, the nickel metal catalyst, the carrier of Al_2O_3, the power was 5W, the gas flow rate was 160 $ml \cdot min^{-1}$, and the nitrogen to hydrogen ratio was 1:2. Under these conditions, the energy efficiency reached 1.49$g \cdot kW \cdot h^{-1}$, an improvement of 22.1% over the previous maximum energy efficiency. The validity of the results is verified by numerical simulation.

3) The results provide an effective experimental design strategy for the plasma-catalyzed ammonia synthesis process and demonstrate the effectiveness of BO in optimizing the parameters of complex experimental systems.

Although studies show that XGBoost and BO are significantly effective in optimizing the experimental parameters of plasma-catalyzed ammonia synthesis, the sample size of the dataset is limited, and the universality of the model still needs further verification. Future studies should consider extending the experimental dataset and adding different types of experimental parameters and scenarios to improve the generalization ability of the model.

Funding

This research was supported by the National Natural Science Foundation of China (52077129); and Shandong Provincial Natural Science Foundation of China (ZR2022ME037).

References

[1] Chavando, J. A. M., Silva, V. B., da Cruz Tarelho, L. A., Cardoso, J. S., Hall, M. J., & Eusébio, D. (2023). Ammonia as an alternative. Combustion Chemistry and the Carbon Neutral Future, 179-208.

[2] Khan, A. R., Al-Awadi, L., & Al-Rashidi, M. S. (2016). Control of ammonia and urea emissions from urea manufacturing facilities of Petrochemical Industries Company (PIC), Kuwait. Journal of the Air & Waste Management Association, 66(6), 609-618.

[3] Wu, G., Geng, J., Xu, K., & Ren, H. (2021). Removal of pharmaceuticals by ammonia oxidizers during nitrification. Applied Microbiology and Biotechnology, 105, 909-921.

[4] Brightling, J. (2018). Ammonia and the fertiliser industry: The development of ammonia at Billingham.

Johnson Matthey Technology Review, 62(1), 32-47.

[5] Valera-Medina, A., Amer-Hatem, F., Azad, A. K., Dedoussi, I. C., De Joannon, M., Fernandes, R. X., ... & Costa, M. (2021). Review on ammonia as a potential fuel: from synthesis to economics. Energy & Fuels, 35(9), 6964-7029.

[6] Chai, W. S., Bao, Y., Jin, P., Tang, G., & Zhou, L. (2021). A review on ammonia, ammonia-hydrogen and ammonia-methane fuels. Renewable and Sustainable Energy Reviews, 147, 111254.

[7] Machaj, K., Kupecki, J., Malecha, Z., Morawski, A. W., Skrzypkiewicz, M., Stanclik, M., & Chorowski, M. (2022). Ammonia as a potential marine fuel: A review. Energy Strategy Reviews, 44, 100926.

[8] Erdemir, D., & Dincer, I. (2021). A perspective on the use of ammonia as a clean fuel: Challenges and solutions. International Journal of Energy Research, 45(4).

[9] Zheng, J., Jiang, L., Lyu, Y., Jiang, S. P., & Wang, S. (2022). Green synthesis of nitrogen-to-ammonia fixation: past, present, and future. Energy & Environmental Materials, 5(2), 452-457.

[10] Santhosh, C. R., & Sankannavar, R. (2023). A comprehensive review on electrochemical green ammonia synthesis: From conventional to distinctive strategies for efficient nitrogen fixation. Applied Energy, 352, 121960.

[11] Wang, B., Zhang, Y., & Minteer, S. D. (2023). Renewable electron-driven bioinorganic nitrogen fixation: a superior route toward green ammonia?. Energy & Environmental Science, 16(2), 404-420.

[12] Bora, N., Singh, A. K., Pal, P., Sahoo, U. K., Seth, D., Rathore, D., ... & Sarangi, P. K. (2024). Green ammonia production: Process technologies and challenges. Fuel, 369, 131808.

[13] Zhao, H., Kamp, L. M., & Lukszo, Z. (2022). The potential of green ammonia production to reduce renewable power curtailment and encourage the energy transition in China. international journal of hydrogen energy, 47(44), 18935-18954.

[14] Ojelade, O. A., Zaman, S. F., & Ni, B. J. (2023). Green ammonia production technologies: A review of practical progress. Journal of Environmental Management, 342, 118348.

[15] El-Shafie, M., & Kambara, S. (2023). Recent advances in ammonia synthesis technologies: Toward future zero carbon emissions. International Journal of Hydrogen Energy, 48(30), 11237-11273.

[16] Humphreys, J., Lan, R., & Tao, S. (2021). Development and recent progress on ammonia synthesis catalysts for Haber–Bosch process. Advanced Energy and Sustainability Research, 2(1), 2000043.

[17] Wang, M., Khan, M. A., Mohsin, I., Wicks, J., Ip, A. H., Sumon, K. Z., ... & Kibria, M. G. (2021). Can sustainable ammonia synthesis pathways compete with fossil-fuel based Haber–Bosch processes?. Energy & Environmental Science, 14(5), 2535-2548.

[18] Erfani, N., Baharudin, L., & Watson, M. (2024). Recent advances and intensifications in Haber-Bosch ammonia synthesis process. Chemical Engineering and Processing-Process Intensification, 109962.

[19] Cheema, I. I., & Krewer, U. (2018). Operating envelope of Haber–Bosch process design for power-to-ammonia. RSC advances, 8(61), 34926-34936.

[20] Niu, X., Shi, A., Sun, D., Xiao, S., Zhang, T., Zhou, Z., ... & Wang, J. (2021). Photocatalytic ammonia synthesis: mechanistic insights into N2 activation at oxygen vacancies under visible light excitation. ACS Catalysis, 11(22), 14058-14066.

[21] Chen, X., Li, N., Kong, Z., Ong, W. J., & Zhao, X. (2018). Photocatalytic fixation of nitrogen to ammonia: state-of-the-art advancements and future prospects. Materials Horizons, 5(1), 9-27.

[22] Zhang, S., Zhao, Y., Shi, R., Waterhouse, G. I., & Zhang, T. (2019). Photocatalytic ammonia synthesis: Recent progress and future. EnergyChem, 1(2), 100013.

[23] Ithisuphalap, K., Zhang, H., Guo, L., Yang, Q., Yang, H., & Wu, G. (2019). Photocatalysis and photoelectrocatalysis methods of nitrogen reduction for sustainable ammonia synthesis. Small Methods, 3(6), 1800352.

[24] Shi, Y., Zhao, Z., Yang, D., Tan, J., Xin, X., Liu, Y., & Jiang, Z. (2023). Engineering photocatalytic ammonia synthesis. Chemical Society Reviews, 52(20), 6938-6956.

[25] Zhao, Z., Ren, H., Yang, D., Han, Y., Shi, J., An, K., ... & Jiang, Z. (2021). Boosting nitrogen activation via bimetallic organic frameworks for photocatalytic ammonia synthesis. ACS Catalysis, 11(15), 9986-9995.

[26] Yang, B., Ding, W., Zhang, H., & Zhang, S. (2021). Recent progress in electrochemical synthesis of ammonia from nitrogen: strategies to improve the catalytic activity and selectivity. Energy & Environmental Science, 14(2), 672-687.

[27] Manjunatha, R., & Schechter, A. (2018). Electrochemical synthesis of ammonia using ruthenium–platinum alloy at ambient pressure and low temperature. Electrochemistry Communications, 90, 96-100.

[28] Yao, Y., Wang, J., Shahid, U. B., Gu, M., Wang, H., Li, H., & Shao, M. (2020). Electrochemical synthesis of ammonia from nitrogen under mild conditions: current status and challenges. Electrochemical Energy Reviews, 3, 239-270.

[29] Wu, T., Fan, W., Zhang, Y., & Zhang, F. (2021). Electrochemical synthesis of ammonia: Progress and challenges. Materials Today Physics, 16, 100310.

[30] Yang, J., Weng, W., & Xiao, W. (2020). Electrochemical synthesis of ammonia in molten salts. Journal of Energy Chemistry, 43, 195-207.

[31] Kyriakou, V., Garagounis, I., Vasileiou, E., Vourros, A., & Stoukides, M. (2017). Progress in the electrochemical synthesis of ammonia. Catalysis Today, 286, 2-13.

[32] Peng, P., Chen, P., Schiappacasse, C., Zhou, N., Anderson, E., Chen, D., ... & Ruan, R. (2018). A review on the non-thermal plasma-assisted ammonia synthesis technologies. Journal of cleaner production, 177, 597-609.

[33] Carreon, M. L. (2019). Plasma catalytic ammonia synthesis: state of the art and future directions. Journal of Physics D: Applied Physics, 52(48), 483001.

[34] Zhu, X., Liu, J., Hu, X., Zhou, Z., Li, X., Wang, W., ... & Tu, X. (2022). Plasma-catalytic synthesis of ammonia over Ru-based catalysts: Insights into the support effect. Journal of the Energy Institute, 102, 240-246.

[35] Hosseini, H. (2023). Dielectric barrier discharge plasma catalysis as an alternative approach for the synthesis of ammonia: a review. RSC advances, 13(40), 28211-28223.

[36] Kim, H. H., Teramoto, Y., Ogata, A., Takagi, H., & Nanba, T. (2017). Atmospheric - pressure nonthermal plasma synthesis of ammonia over ruthenium catalysts. Plasma Processes and Polymers, 14(6), 1600157.

[37] Sun, J., Chen, Q., Zhao, X., Lin, H., & Qin, W. (2022). Kinetic investigation of plasma catalytic synthesis of ammonia: insights into the role of excited states and plasma-enhanced surface chemistry. Plasma Sources Science and Technology, 31(9), 094009.

[38] Rouwenhorst, K. H., Engelmann, Y., van't Veer, K., Postma, R. S., Bogaerts, A., & Lefferts, L. (2020). Plasma-driven catalysis: green ammonia synthesis with intermittent electricity. Green chemistry, 22(19), 6258-6287.